Journal of Research in Pharmacy

Research Article

www.jrespharm.com

Improve the solubility of cefpodoxime proxetil by amorphous solid dispersion technique

Ali Mohammed HUSSEIN[1] *, Ghaidaa S. HAMEED[1], Fitua M. AZIZ [2]

[1] Department of Pharmaceutics, College of Pharmacy, Mustansiriyah University, Baghdad, Iraq
[2] Department of Clinical Laboratory Sciences, College of Pharmacy, Mustansiriyah University, Baghdad, Iraq.
* Corresponding Author. E-mail: amh.iraq821@uomustansiriyah.edu.iq (A.H.); Tel. +964 790 163 9295.

Received: 15 July 2024 / Revised: 17 August 2024 / Accepted: 20 August 2024

ABSTRACT: This research aimed to improve the solubility and stabilize cefpodoxime proxetil (CP), a class IV drug, by amorphous solid dispersion (ASD) technique. Four formulations were prepared by dispersing amorphous CP in soluplus, polyvinylpyrrolidone (PVP K30), and ethyl cellulose (EC) blends in different compositions and ratios. The optimum formulation was stored in accelerated conditions at 40 °C and 75% relative humidity for six months. The drug's solubility and dissolution rate in different systems were explored. Furthermore, Differential Scanning Calorimetry (DSC), X-ray Powder Diffractometry (PXRD), Fourier Transform Infrared spectroscopy (FTIR), and Field Emission Scanning Electron Microscopy (FESEM) were used to examine the physical state of the drug. The antibacterial activity of the drug was evaluated during the experiment. When mixing CP with soluplus and PVP K30 in a 1:1:1 ratio as ASD, the drug solubility at pH 1.2 enhanced about 28 folds than a pure drug, and the dissolution rate increment was observed. The DSC, FTIR, and PXRD data confirmed the drug is amorphous and miscible with these polymers. FESEM revealed particle size reduction. The antibacterial activity was raised. After storage in the accelerated condition, physical investigations indicated that no recrystallization occurred, and this condition had little effect on *in vitro* drug dissolution and antibacterial activity. This can be a good indicator of the drug's solubility enhancement and physical stability optimization that will make the possibility of preparing this drug in the future as an oral solid dosage form with the possibility of manufacturing with a drug company due to the promising results.

KEYWORDS: Amorphous solid dispersion (ASD) technique ; cefpodoxime proxetil; physical stability; solubility.

1. INTRODUCTION

Up to 90% of newly approved chemicals and 40% of approved drugs have low aqueous solubility (i.e., The Biopharmaceutical Classification System class II and IV) [1, 2]. These days, a variety of pharmaceutical techniques, such as cocrystal, self-emulsifying drug delivery systems, micronization, nano-crystallization, solvent deposition, complexation, micellar solubilization, pH adjustment, and amorphous solid dispersion (ASD), are used to improve drug solubility and dissolution rate of these drugs [3-6].

Amorphization of these drugs from crystalline to amorphous form increases the solubility. Since the drug does not require energy to break its crystal lattice when it is amorphous [7]. However, because of their excess free energy and enthalpy, these amorphous systems are thermodynamically unstable, which causes relaxation, nucleation, and crystallization during processing, storage, or inside the GI tract, losing their beneficial properties. In general, the amorphous drug can be dispersed in a polymer matrix to increase stability, yielding ASD [8-10].

The choice of polymeric excipient significantly influences both physical stability and dissolution behavior [11]. When compared to neat amorphous drugs, active pharmaceutical ingredients (API) formulated in ASD generally exhibit greater physical stability, and yet their dissolution rate is faster than their crystalline equivalents [12]. Amorphous-amorphous phase separation (AAPS) is when a miscible ASD splits into two phases within the matrix: polymer-rich and drug-rich phases. Although the drug is still amorphous, AAPS causes an acceleration in API recrystallization because drug-rich domains do not have the polymer's stabilizing effect [13-16]. However, recrystallization eliminates the amorphous system solubility benefit [17]. Furthermore, both solvent-based and fusion-based methods can be used to generate ASD.

How to cite this article: Hussein AM, Hameed GS, Azız FM. Improve the solubility of cefpodoxime proxetil by amorphous solid dispersion. J Res Pharm. 2025; 29(4): 1437-1450.

ISSN: 2630-6344

https://dx.doi.org/10.12991/jrespharm.1734450

Specific mechanical procedures, such as grinding or ball milling, can also cause some amorphization [18, 19].

First-generation solid dispersions made using crystalline polymers have the disadvantage of sluggish drug release because of their crystalline form. Higher solubility and dissolution were obtained by using amorphous polymers; these ASDs were referred to as second-generation solid dispersions. The drug precipitation and recrystallization during storage are the limits of these ASDs. Third-generation ASDs were created to get around these restrictions by adding another polymer and/or surfactants to enhance stability and dissolution to a greater extent [20-22]. Compared to binary composition, a ternary system containing two suitably distinct polymers can work in concert to promote solubility, maintain a supersaturated state, reduce molecular mobility, form drug-polymer-polymer interactions, and reduce overall hygroscopicity [23-25].

The body's drug concentration determines its pharmacological effects. An amorphous solid increases the drug's aqueous solubility, improving its oral bioavailability and antibacterial activity. The possibility of amorphous API recrystallization in solid dispersion could decrease the dissolution rate and a consequent decrease in antibacterial activity due to low exposure levels (bioavailability) [26-28].

Cefpodoxime proxetil (CP) is a third-generation cephalosporin that is effective for treating Gram-positive and Gram-negative bacterial infections involving skin, urinary tract, respiratory, and gonorrhea infections. It treats community-acquired pneumonia caused by *Haemophilus influenzae* or *Salmonella pneumonia* [29, 30]. CP is a class IV with a Tg of 98.79 °C. It is a weak base that exhibits a pH-dependent solubility (pka is around 2.2), making it soluble in acidic solution but weakly soluble in alkaline solution [31-35]. Even though amorphous CP is an esterified prodrug that increases cefpodoxime's permeability, its oral bioavailability is still limited [36, 37]. The drug bioavailability is about 50%, and it is primarily attributed to the pre-absorption intestinal breakdown of CP's ester side chain by cholinesterase digestive enzymes into cefpodoxime. CP limited bioavailability is also attributed to its poor water solubility, characteristic gelation behavior, and total degradation in alkaline conditions. Since about 55% of its content degraded in 8 hours (hrs) at pH 6.8, and it completely degraded to CA in 24 hrs [38-45].

According to the previous study, saturated aqueous solubility, dissolution rate, and antibacterial activity were improved by formulating CP with Pluronic® F127 / Polyvinylpyrrolidone (PVP K30) as ASD. It was shown by an increase in solubility from 3.5 to 8 times [46]. Another study demonstrated that CP's solubility and dissolution rate were increased when it was prepared as an ASD utilizing the solvent dispersion method with skimmed milk powder as the carrier. The formulations showed acceptable physico-chemical parameters for two months and were stable [47].

The objective of this study was to improve the solubility of CP by amorphous solid dispersion technique using soluplus, PVP K30, and ethyl cellulose (EC) in different compositions and ratios and investigate the physical stability of the best formulation during six months of storage at accelerated condition (40 °C and 75% relative humidity (RH) according to The International Council for Harmonisation of Technical Requirements for Pharmaceuticals for Human Use (ICH) Guideline) by DSC, PXRD, FTIR, FESEM, *in vitro* release, and antibacterial zone of inhibition.

2. RESULTS AND DISCUSSION

2.1. Saturation solubility study

Table 1 provides the data for the saturation solubility study results. It showed that the drug's solubility is pH-dependent, meaning the drug's solubility fell when PH rose. After preparation of ASD, at PH 1.2, F1 improved the solubility more than F since F1 inclined the solubility approximately 28 times compared with F, which raised the solubility around five times. F2 showed a little decline in the solubility, while F3 did not affect the solubility. On the other hand, none of these formulations could enhance the solubility and could not protect the drug from degradation at PH 4.6 and 7.4 after 72 hrs. It suggested that chemical instability was attributed to the drug-polymer bonding not being enough to negate CP degradation in the neutral and alkaline solution.

Table 1. Saturation solubility study of CP, F (CP:soluplus 1:1), F1 (CP:soluplus:PVP 1:1:1), F2 (CP:PVP 1:2) and F3 (CP:PVP:EC 1:1.5:0.5) (mean ± SD, n=3)

Formulation	PH 1.2 (mg/ml)	PH 4.6 (mg/ml)	PH 7.4 (mg/ml)
CP	5.542±0.164	0.581±0.084	0.562±0.048
F	25.003±0.509	0.341±0.388	0.651±0.087
F1	142.061±0.44	0.626±0.02	0.638±0.049
F2	5.384±0.232	0.922±0.266	1.148±0.136
F3	5.928±0.12	0.97±0.076	2.466±0.392

2.2. Differential scanning calorimetry (DSC)

DSC is one of the most valuable techniques for thermal analysis to determine a drug's thermal behavior. Figure 1 displays the thermogram for both pure drug and ASD formulations. However, CP had Tg 99.69 °C. Since no sharp peak was observed, elucidated the amorphous state of the drug and is compatible with Mujtaba *et al*. result who reported that CP did not show any sharp melting endotherm between 40 °C and 200 °C [48]. Furthermore, all ASD formulations have shown similar patterns, and a single Tg was obtained for each formulation, indicating that the drug is miscible with these polymers and confirming the successful formation of amorphous systems. These results were in agreement with the data reported by Patel *et al* who demonstrated that DSC thermograms of the hot melt extrudate after blending CP with Eudragit did not show melting endotherm) [49].

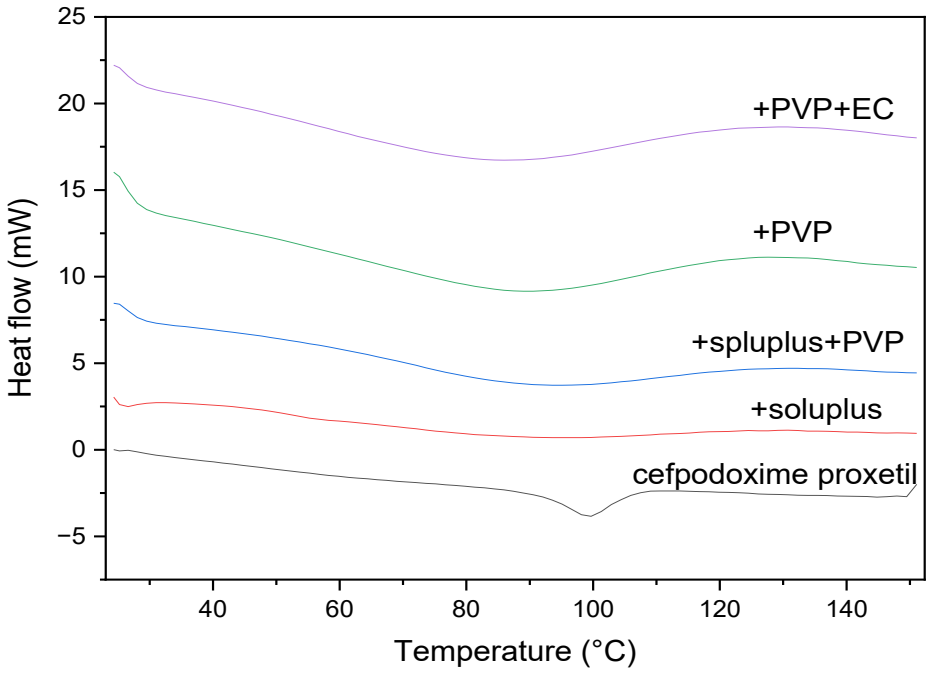

Figure 1. The DSC thermogram of CP, F (CP:soluplus 1:1), F1 (CP:soluplus:PVP 1:1:1), F2 (CP:PVP 1:2) and F3 (CP:PVP:EC 1:1.5:0.5)

2.3. Fourier transforms infrared spectroscopy (FTIR)

FTIR spectroscopy was used to investigate the possibility of intermolecular interaction between the drug and polymers [50]. The FTIR spectra of CP showed wavenumber of 3341 cm^{-1} for N-H vibration, 2985 cm^{-1} and 2939 cm^{-1} for C-H vibration, 1759 cm^{-1} for C=O vibration, 1681 cm^{-1} for C=O vibration, 1539 cm^{-1} for C=C vibration, 1454 cm^{-1} for C=N vibration, 1373 cm^{-1} for C=C vibration, 1273 cm^{-1} for C–N vibration, and 1072 cm^{-1}. for C–C vibration, 902 cm^{-1} for C-CL vibration and 810 cm^{-1} for C-H vibration (Figure 2) [51].

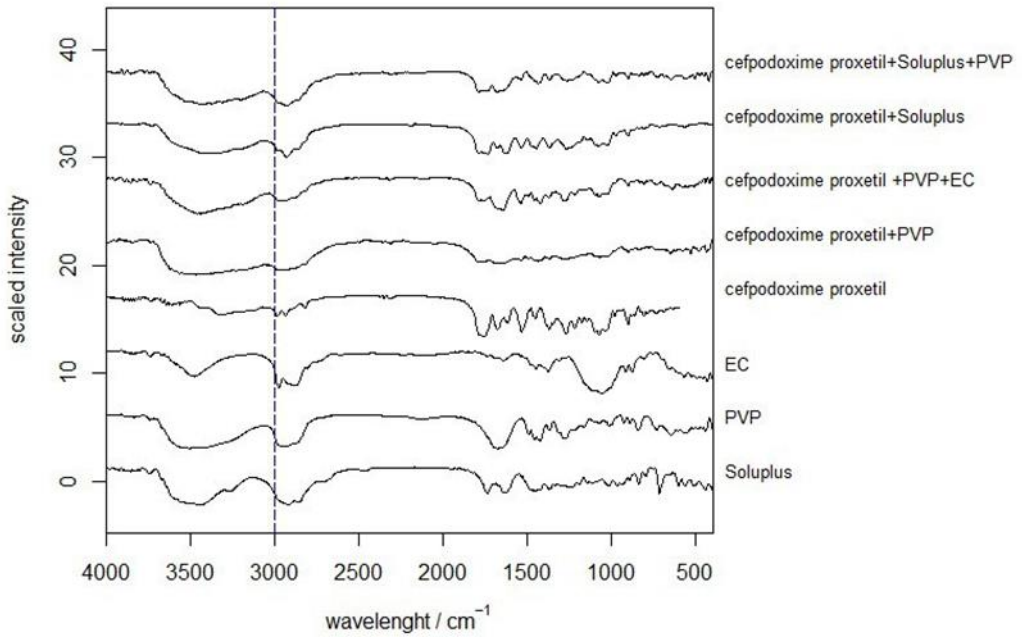

Figure 2. FTIR spectra of soluplus, PVP, EC, CP, F (CP:soluplus 1:1), F1 (CP:soluplus:PVP 1:1:1), F2 (CP:PVP 1:2) and F3 (CP:PVP:EC 1:1.5:0.5)

Compared to the neat amorphous API, the FTIR spectrum of ASD formulations obtained showed several significant differences (Table 2). F, F1, F2, and F3 peaks corresponding to the N-H vibration at a wavenumber of 3321 cm^{-1} were significantly broadened and shifted to the higher wavenumber. In addition, peaks at wavenumber of 2985 cm^{-1} corresponding to the C-H vibration lower shifted in these formulations. Whereas there was a significant peak intensity reduction and higher shift corresponding to the C=O vibration at a wavenumber of 1759 cm^{-1} except F, where this peak is lower shifted and stilled with the same intensity. The polymers' miscibility with CP is shown by peak shifting, broadening, and intensity reduction, which were indicative of hydrogen-bonding interactions as seen in Kader *et al*. experiment [52]. The evidence suggests that the hydrogen bonding with the C-H group CP molecule may be sufficiently strong to weaken the N-H stretching, resulting in a weak and broad peak.

Table 2. Wavenumber of the characteristic peaks of CP and ASD formulations

Formulation	N-H vibration (cm^{-1})	C-H vibration (cm^{-1})	C=O vibration (cm^{-1})
CP	3321	2985	1759
F	3421	2931	1739
F1	3437	2931	1789
F2	3502	2974	1789
F3	3460	2981	1789

2.4. Powder X-ray Diffraction (PXRD)

The drug's crystallinity change might be investigated using XRPD. The X-ray diffractogram of CP showed a typical halo peak, indicating an overall amorphous form (Figure 3) [43]. After preparation of the F1 formulation, the drug was still amorphous without Braggs along the peak, which is identical to the work done by Duraivel *et al*. [53] The outcomes of this experiment confirmed the results of DSC studies.

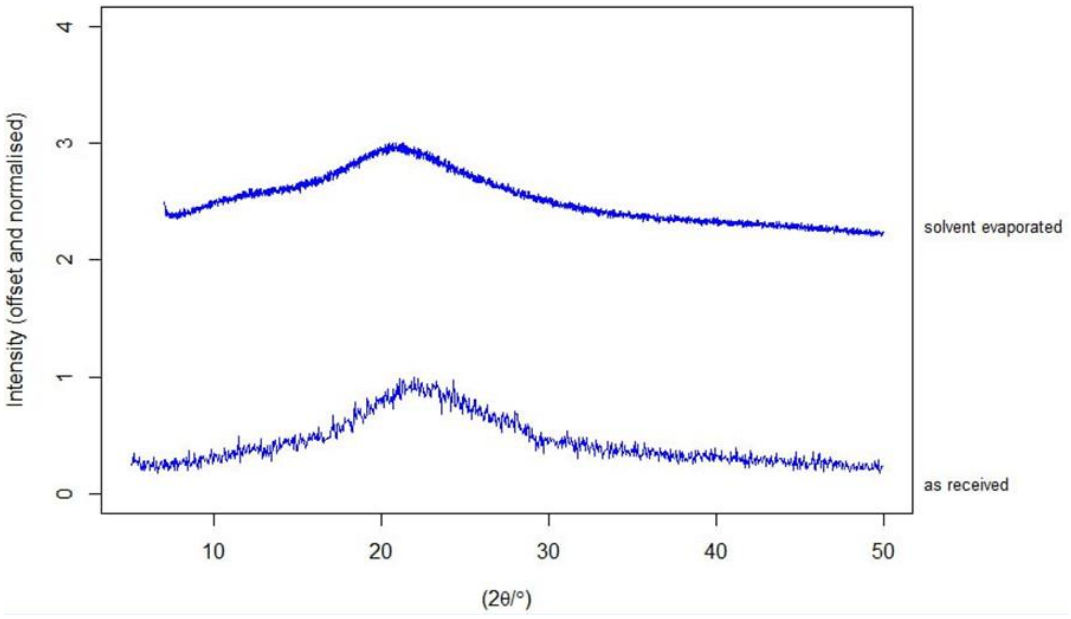

Figure 3. The PXRD diffractogram of CP and F1 (CP:soluplus:PVP 1:1:1) formulation

2.5. Field Emission Scanning Electron Microscope (FESEM)

Large particles of CP with particle size around 106.2 nm, sticky and hazy structures were seen (Figure 4). However, the change in surface morphology showed a fine and fluffy state and a smaller particle size of about 35.02 nm, observed in the F1 formulation.

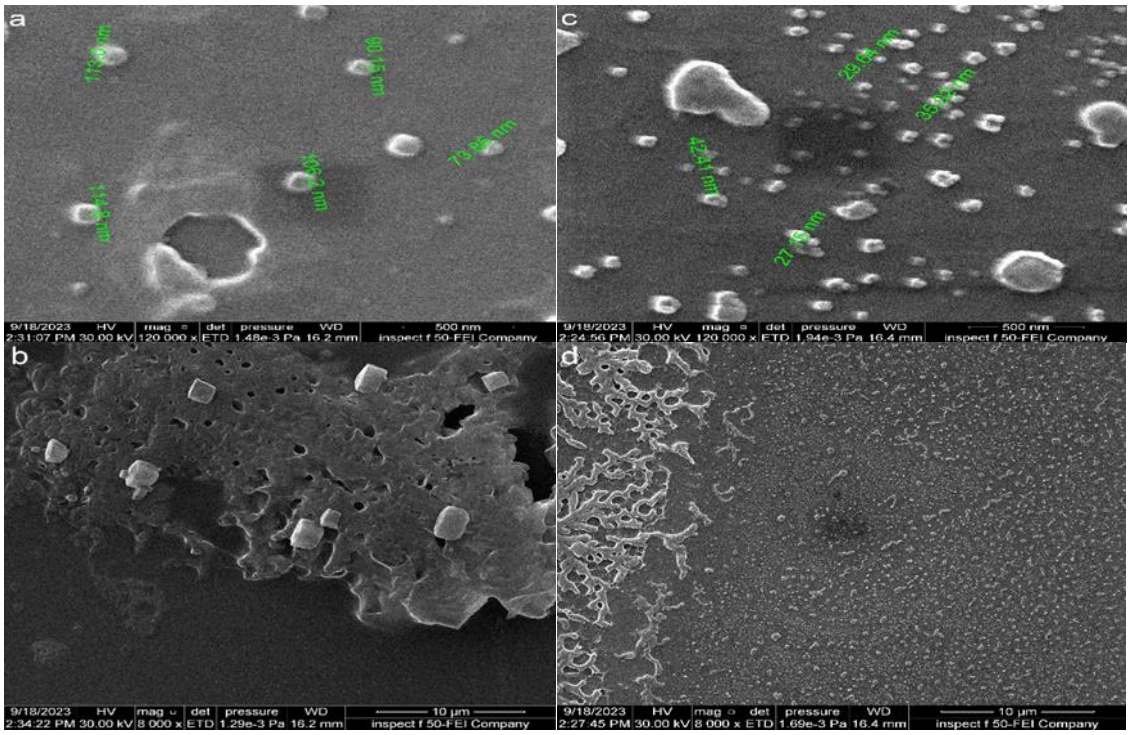

Figure 4. FESEM micrographs of CP (a and b) and F1 (CP:soluplus:PVP 1:1:1) formulation (c and d)

2.6. *In vitro* dissolution study

Dissolution studies were conducted to investigate the dissolution performance of the pure drug and various ASD formulations in HCL 0.1N (PH 1.2) for up to 120 minutes (min). Figure 5 demonstrates that the

initial cumulative drug release in an acidic solution is around 69 % at 15 min. After that, the cumulative drug release of CP elevates slowly to reach about 78%. This was well-matched to the results of Fan *et al*. [54].

F1, F2, and F3 accelerated initial cumulative drug release, whereas F slowed it below API value in the same period. Later, the cumulative drug release of all ASD formulations exceeded the CP value to the range between (85-100%) at the end of 120 min. It means the dissolution rate of CP was enhanced with F1, F2, and F3, and the solution concentrations of the drug with all formulations were higher than amorphous CP, resulting from an increased wettability and supersaturation maintenance in addition to particle size reduction.

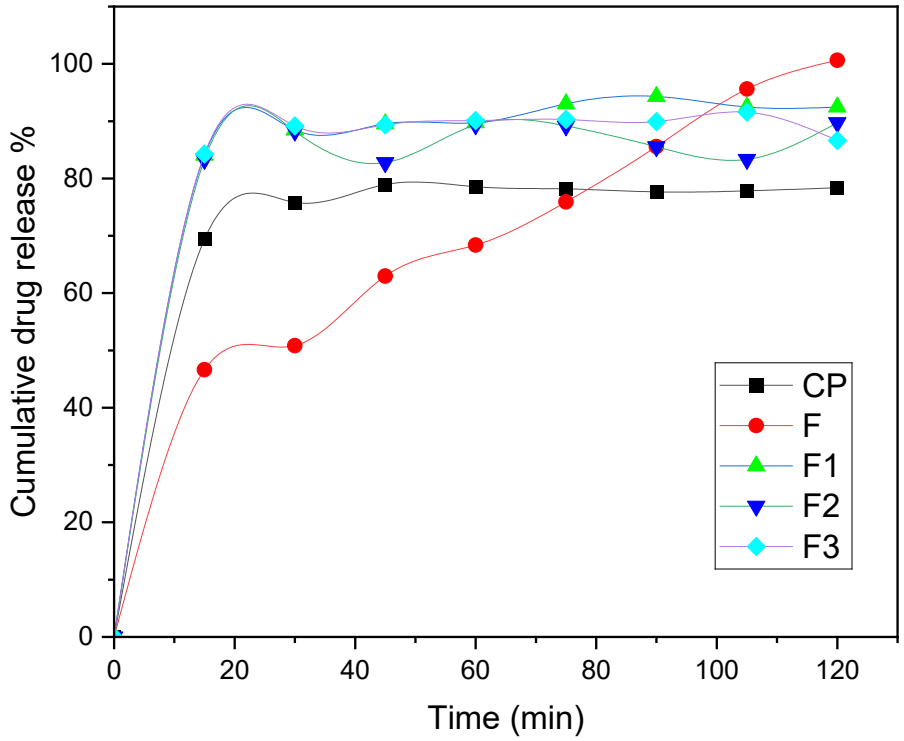

Figure 5. Dissolution profile of CP, F (CP:soluplus 1:1), F1 (CP:soluplus:PVP 1:1:1), F2 (CP:PVP 1:2) and F3 (CP:PVP:EC 1:1.5:0.5) (mean ± SD, n=3)

2.7. Antibacterial activity

The goal of antibacterial studies was to determine the effect of drug solubility on its efficacy in inhibiting the growth of pathogenic bacteria. Table 3 shows the antibacterial activity of 500 mcg/ml of CP against the two tested bacteria. The released drug from F and F1 inhibited bacterial growth more effectively than the pure drug, F2 and F3, demonstrating the potential of this formulation to treat illnesses caused by these bacteria (Figure 6).

Table 3. Antibacterial activity of the CP and ASD formulations (mean ± SD, n=3)

Formulation	Inhibition zone mean (mm) ± SD	
	P. mirabilis	*S. pneumoniae*
CP	19.66±0.57	13.33±1.52
F	23±1	20±1
F1	25.33±1.52	20.66±1.15
F2	20.33±0.57	15.33±0.57
F3	21.66±1.15	14.66±0.57

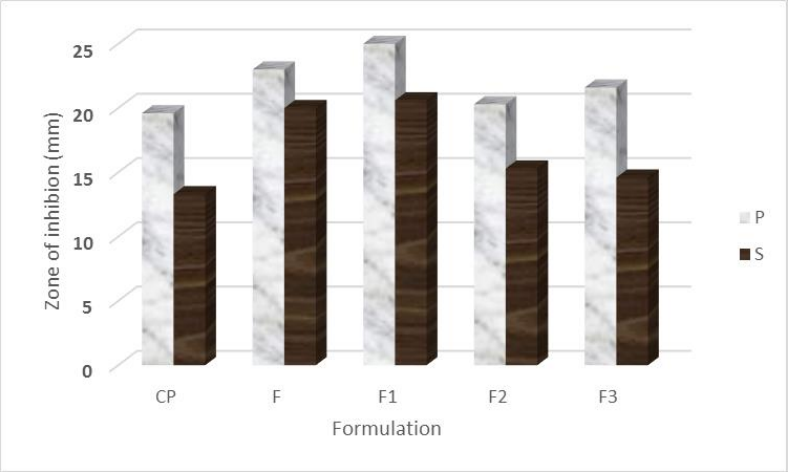

Figure 6. The antibacterial activity of CP, F (CP:soluplus 1:1), F1 (CP:soluplus:PVP 1:1:1), F2 (CP:PVP 1:2), and F3 (CP:PVP:EC 1:1.5:0.5) against *P. mirabilis* and *S. pneumoniae* (mean ± SD, n=3)

F1 had the best results among other formulations in the above experiments. Since the solubility of CP raised around 28 times in the saturation solubility test, the cumulative drug release inclined about 14 % (p-value <0.05) with antibacterial activity improvement. So, this composition was predicted to be an optimum formulation to submit for the stability test.

2.8. Stability study

The F1 sample exhibited a single Tg value during this period, suggesting homogeneity and the absence of AAPS. In addition, it didn't display any sharp endothermic peak in which CP was still stable against recrystallization during the sixth month of storage (Figure 7).

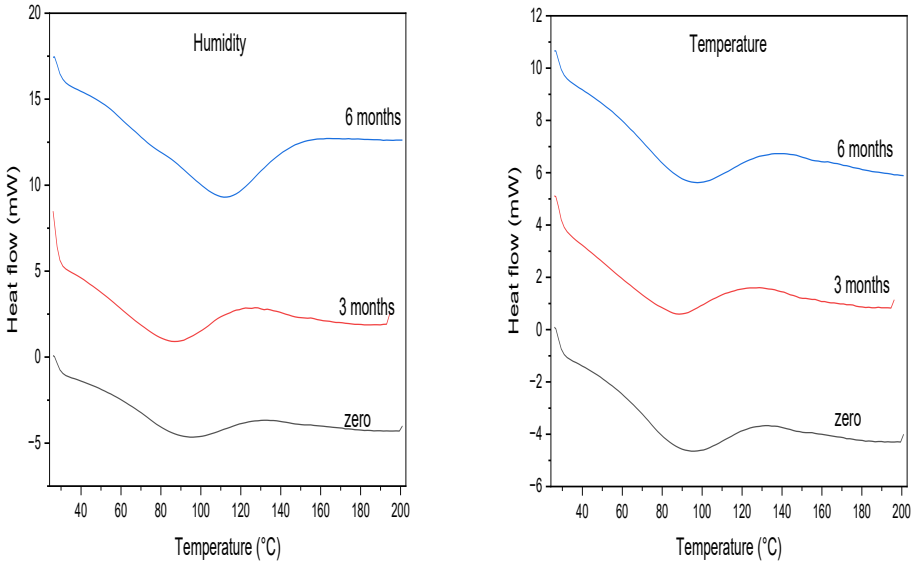

Figure 7. The DSC thermogram of F1 (CP:soluplus:PVP 1:1:1) after zero, 3, and 6 months of storage at 75%RH and 40 °C

FTIR spectrum of F1 exhibits notable changes in intensity and peak shape over six months when stored at higher temperatures and humidity levels (Figure 8). Besides, the peak corresponding to the N-H shifted higher in the first and third months. This peak shifted to a lower wavenumber in other months. But peaks of C-H and C=O groups stilled within the range even stored for 180 days. Since there was little or no peak shifting in this period,

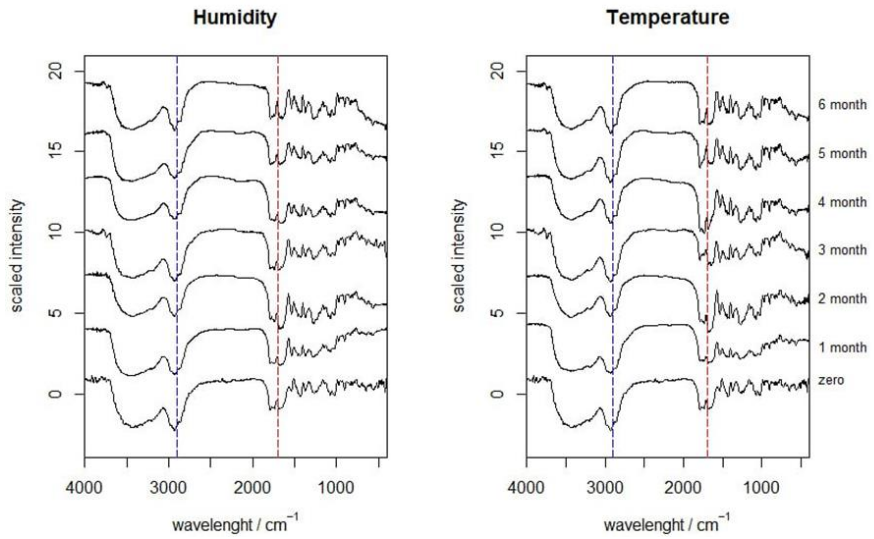

Figure 8. The FTIR spectra of F1 (CP:soluplus:PVP 1:1:1) after zero, 1, 2, 3, 4, 5, and 6 months of storage at 75%RH and 40 °C

It was observed that all of the characteristic peaks associated with the drug were retained, and the absence of new peaks (approximately 3583 cm^{-1}) in the FTIR spectra of F1 formulation indicated that no new compound (recrystallization to cefpodoxime acid) was generated during storage and confirmed its stability in the accelerated condition [12, 55].

When F1 samples were kept under accelerated conditions, it was noted that they were found to be ultimately halos and didn't undergo recrystallization under these conditions for up to 3 months (Figure 9). Also, the diffractogram revealed that the F1 formulation was mostly amorphous, with no diffraction Braggs observed in the second half of the storage period. Moreover, the X-ray data showed no indication of AAPS. Since the positions of the X-ray amorphous halos did not change with time [56]. It was also agreed with DSC and FTIR results.

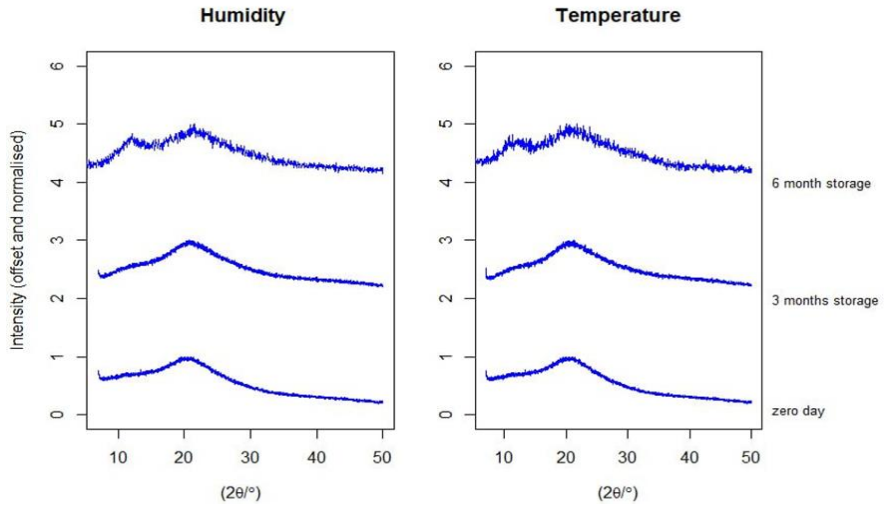

Figure 9. The PXRD diffractogram of F1 (CP:soluplus:PVP 1:1:1) after zero, 3, and 6 months of storage at 75% RH and 40 °C

Figure 10 displayed the F1 samples' dissolution profile during six months of storage under accelerated conditions. During the first three months of storage, F1 samples displayed drug release, the same as its release from the immediately prepared formulation under both conditions, confirming the amorphous form of CP. Meanwhile, the drug release from F1 saw a slight delay within the first hour of the last three months of storage. However, at the end of the second hour, it nearly reached 92%. It demonstrates that F1 formulation may prevent amorphous CP from recrystallizing even after exposure to harsh conditions for a long time

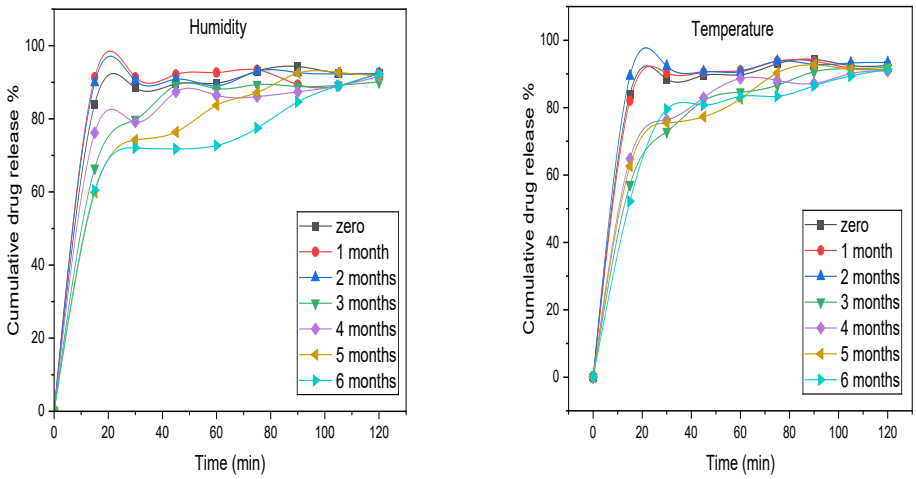

Figure 10. The dissolution profile of F1 (CP:soluplus:PVP 1:1:1) after zero, 1, 2, 3, 4, 5, and 6 months of storage at 75%RH and 40 °C (mean ± SD, n=3)

Furthermore, microbiological evaluation studies during six months of storage demonstrate that F1 gave approximately the same diameters compared with recently prepared formulation against both bacteria, which means this composition upsurges and preserves the antibacterial activity of the drug after exposure to a half year of harsh conditions (Figure 11).

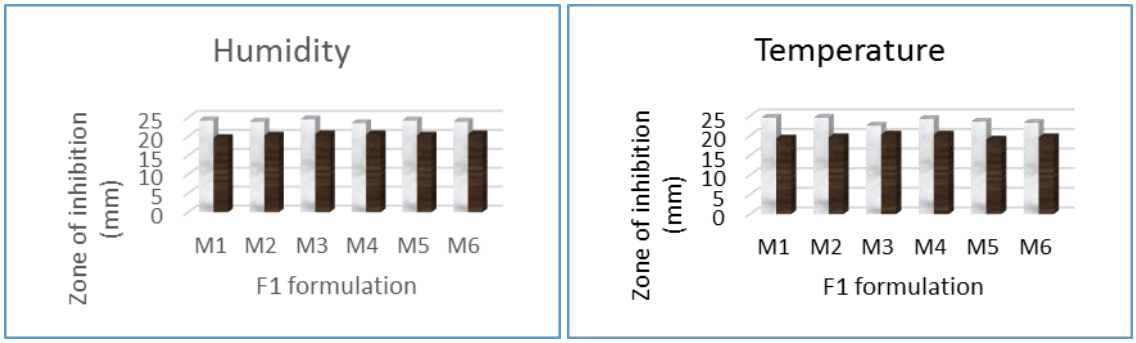

Figure 11. Antibacterial activity of F1 (CP:soluplus:PVP 1:1:1) after 1, 2, 3, 4, 5, and 6 months of storage at 75% RH and 40 °C (mean ± SD, n=3)

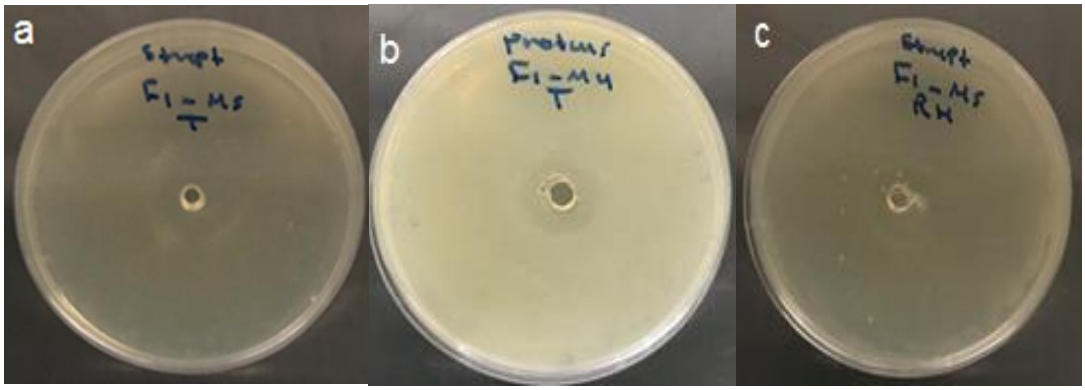

Figure 12. The agar plates show a zone of inhibition around the wells for formulation F1 (CP:soluplus:PVP 1:1:1) against a) *S. pneumoniae* after storage at 40 °C for five months b) *P. mirabilis* after storage at 40 °C for four months c) *S. pneumoniae* after storage at 75% RH for five months.

3. CONCLUSION

The significant solubility enhancement of pure drug was observed in the F1 formulation, and it was attributed to the wetting effect and supersaturation maintenance of polymers in addition to the particle size reduction by the solid dispersion technique. The stability studies showed no or little changes (neither AAPS nor recrystallization) were recorded concerning F1 in harsh conditions over six months. Therefore, the corporation of low hygroscopic soluplus and PVP k30 with antiplasticizing effect, in addition to their strong hydrogen bonding interaction, made this ternary system effectively improve the solubility and optimized the physical stability of the amorphous CP in accelerated condition.

4. MATERIALS AND METHODS

4.1. Materials

CP was supplied by the Hubei Widlely Chemical Reagent Co., Ltd., (Wuhan, China). Soluplus® (MW: 118,000 g/mol) was purchased by BASF (Ludwigshafen, Germany). PVP K30 (MW: 40,000 g/mol) was obtained from CDH (P) Ltd. (Delhi, India). EC was bought from HIMedia Laboratories Pvt. Ltd (Maharashtra, India). All other chemicals were of analytical grade.

4.2. Preparation of amorphous solid dispersion

The composition of the different ASD systems prepared by the solvent evaporation method is given in Table 4. After dissolving CP, PVP K30, Soluplus, and EC in methanol, the solvent was evaporated using a rotary evaporator (BUCHI Rotavapor R-205) from Switzerland. The dried film that was thus produced was then passed through a sieve no. 40 and dried again at 25 °C [57].

Table 4. ASD formulations

Formulation	Composition	Drug to polymer molar ratio
F	CP-soluplus	1:1
F1	CP-PVP K30-soluplus	1:1:1
F2	CP-PVP K30	1:2
F3	CP-PVP K 30-EC	1:1:0.5

4.3. Determination of the saturation solubility

The investigation focused on the equilibrium solubility of CP and ASD formulations in different PH solutions. In summary, the excess samples were dispersed in 10 mL solutions with PH values of 1.2, 4.6, and 7.4. The suspension was then stirred at 100 rpm under 37 °C. After 72 hrs, a 0.45 µm syringe filter was used to filter the solution. The filtrates were then examined using a UV-1800 spectrometer (Shimadzu, Japan) at 263.5, 231.5, and 232.5 nm [58].

4.4. Differential Scanning Calorimetry (DSC)

Powder samples were subjected to thermodynamic analysis using DSC (Shimadzu, Japan). Weighed 3-5 mg powder samples were put in an aluminum-sealed pan. During the sample scanning, a heating rate of 10 °C/min from 30 °C to 200 °C in an atmosphere of nitrogen was used. The endothermic peak of the DSC curve was used to record their Tg.

4.5. Fourier Transforms Infrared Spectroscopy (FTIR)

The drug, polymers, and ASD formulations were all the subject of FTIR analyses. The materials were combined with KBr and tableted before being analyzed using FTIR (Shimadzu, Japan). Using a 4 cm^{-1} solution, the scans were taken between the 4000–400 cm^{-1} scanning wavenumber ranges.

4.6. Powder X-ray Diffraction (PXRD)

Powder sample PXRD patterns were obtained with an X-ray diffractometer. The working condition were as follows: voltage of 40 kV, current of 30 mA, and scanning speed of 1/min across a range of 10–90° (2θ).

4.7. Field Emission Scanning Electron Microscope (FESEM)

The surface morphology was investigated at different resolutions using a FESEM (Inspect F 50, FEI company, Spain). After the samples were air-dried and fixed on double-sided adhesive tape previously secured to glass stubs, the stub was put into a fine coat ion sputter for gold coating, and the pure drug and F1 surface morphology were examined.

4.8. *In vitro* dissolution study

A USP II apparatus was used in the dissolution investigation, conducted at 37 ± 0.5 °C and 100 rpm paddle speed utilizing the paddle method. To put it briefly, 900 mL of 0.1N HCL with PH 1.2 was used as the dissolution media, and the proper quantity of the drug and ASD samples (equal to 100 mg of CP) were added. Periodically, samples (5 mL) were taken, and an equivalent volume of dissolution media was added. The concentration of CP was measured at 263.5 nm using a UV-1800 spectrometer (Shimadzu, Japan) following filtering through a 0.45 µm syringe filter.

4.9. Antibacterial activity

Mueller-Hinton agar was utilized as a culture-growing medium. It was prepared by the manufacturer's specifications and autoclaved for 15 min at 121 °C and 15 psi of pressure. The medium was left to solidify after being transferred onto sterile Petri dishes. Using the agar well diffusion technique, the in vitro antibacterial activity of CP and ASD formulations was tested against Gram-negative *Proteus mirabilis (P. mirabilis)* and Gram-positive *Streptococcus pneumoniae (S. pneumoniae)*. A 0.5 McFarland standard, which has an optical density comparable to a bacterial suspension density of 1.5 x 108 colony-forming units (CFU/ml), was used to compare the density of cultured bacteria. Bores were made into the solidified material using a sterile borer. After passing through a 0.45 µm syringe filter, 0.1 ml of Sample solutions with CP concentration in 0.1N HCL (500 mcg/ml) were added to the appropriate bores to permit diffusion and settling. Samples from petri plates were placed in an incubator at 37 °C for a whole day. Following this, the zone of inhibition was determined [59].

4.10. Accelerated stability study

Under specific storage conditions (25 °C and 60% RH for two years or 40 °C and 75% RH for six months, according to ICH Guidelines), stability studies must be conducted to confirm the formulations' physical stability against AAPS and undesired recrystallization [16, 60-62]. Physical stability of optimum formulation was examined after storing the optimum formulation for six months at 40 °C in an incubator and at 75% RH in a desiccator. Samples were taken monthly, and their stability was assessed by DSC, PXRD, FTIR, *in vitro* release, and antibacterial zone of inhibition.

4.11. Statistical analysis

All of the data are shown as mean ± standard deviation (SD). A one-way ANOVA with the Prism software was used to establish the statistical significance. A significant p-value of <0.05 was considered [63,64].

Author contributions: Concept – G.H., F.A.; Design – G.H., F.A.; Supervision – G.H., F.A.; Resources – A.H.; Materials – A.H.; Data Collection and/or Processing – A.H.; Analysis and/or Interpretation – A.H., G.H.; Literature Search – A.H.; Writing – A.H., G.H.; Critical Reviews – G.H., F.A.

Conflict of interest statement: The authors declared no conflict of interest" in the manuscript.

REFERENCES

[1] Solomon S, Iqbal J, Albadarin AB. Insights into the ameliorating ability of mesoporous silica in modulating drug release in ternary amorphous solid dispersion prepared by hot melt extrusion. Eur J Pharm Biopharm. 2021;165:244-258. https://doi.org/10.1016/j.ejpb.2021.04.017

[2] Pignatello R, Corsaro R, Bonaccorso A, Zingale E, Carbone C, Musumeci T. Soluplus® polymeric nanomicelles improve solubility of BCS-class II drugs. Drug Deliv Transl Res. 2022;12(8):1991-2006. https://doi.org/10.1007/s13346-022-01182-x

[3] Han R, Xiong H, Ye Z, Yang Y, Huang T, Jing Q, Lu J, Pan H, Ren F, Ouyang D. Predicting physical stability of solid dispersions by machine learning techniques. J Control Release. 2019;311:16-25. https://doi.org/10.1016/j.jconrel.2019.08.030

[4] Kim J-S, Park H, Kang K-T, Ha E-S, Kim M-S, Hwang S-J. Micronization of a poorly water-soluble drug, fenofibrate, via supercritical-fluid-assisted spray-drying. J Pharm Investig. 2022;52(3):353-366. http://dx.doi.org/10.1007/s40005-022-00565-z

[5] Quan W, Kong S, Ouyang Q, Tao J, Lu S, Huang Y, Li S, Luo H. Use of 18β-glycyrrhetinic acid nanocrystals to enhance anti-inflammatory activity by improving topical delivery. Colloids Surf B Biointerfaces. 2021;205:111791. https://doi.org/10.1016/j.colsurfb.2021.111791

[6] Tekade AR, Yadav JN. A review on solid dispersion and carriers used therein for solubility enhancement of poorly water soluble drugs. Adv Pharm Bull. 2020;10(3):359-369. https://doi.org/10.34172%2Fapb.2020.044

[7] Suresh K, Matzger AJ. Enhanced drug delivery by dissolution of amorphous drug encapsulated in a water unstable metal–organic framework (MOF). Angew Chem Int Ed. 2019;58(47):16790-16794. https://doi.org/10.1002/anie.201907652

[8] Bhanderi A, Bari F, Al-Obaidi H. Evaluation of the impact of surfactants on miscibility of griseofulvin in spray dried amorphous solid dispersions. J Drug Deliv Sci Technol. 2021;64:102606. http://dx.doi.org/10.1016/j.jddst.2021.102606

[9] Bansal SS, Kaushal AM, Bansal AK. Enthalpy relaxation studies of two structurally related amorphous drugs and their binary dispersions. Drug Dev Ind Pharm. 2010;36(11):1271-1280. https://doi.org/10.3109/03639041003753847

[10] Czajkowski M, Jacobsen A-C, Bauer-Brandl A, Brandl M, Skupin-Mrugalska P. Hydrogenated phospholipid, a promising excipient in amorphous solid dispersions of fenofibrate for oral delivery: Preparation and in-vitro biopharmaceutical characterization. Int J Pharm. 2023; 644:123294. https://doi.org/10.1016/j.ijpharm.2023.123294

[11] Lehmkemper K, Kyerematen SO, Bartels M, Degenhardt M, Sadowski G. Physical stability of API/polymer-blend amorphous solid dispersions. Eur J Pharm Biopharm. 2018;124:147-157. https://doi.org/10.1016/j.ejpb.2017.12.002

[12] Lust A, Strachan CJ, Veski P, Aaltonen J, Heinämäki J, Yliruusi J, Kogermann K. Amorphous solid dispersions of piroxicam and Soluplus®: Qualitative and quantitative analysis of piroxicam recrystallization during storage. Int J Pharm. 2015;486(1-2):306-314. https://doi.org/10.1016/j.ijpharm.2015.03.079

[13] Trasi NS, Bhujbal SV, Zemlyanov DY, Zhou QT, Taylor LS. Physical stability and release properties of lumefantrine amorphous solid dispersion granules prepared by a simple solvent evaporation approach. Int J Pharm X. 2020 ;2:100052. https://doi.org/10.1016/j.ijpx.2020.100052

[14] Kawakami K, Bi Y, Yoshihashi Y, Sugano K, Terada K. Time-dependent phase separation of amorphous solid dispersions: Implications for accelerated stability studies. J Drug Deliv Sci Technol. 2018;46:197-206. http://dx.doi.org/10.1016/j.jddst.2018.05.016

[15] Yang R, Zhang GG, Kjoller K, Dillon E, Purohit HS, Taylor LS. Phase separation in surfactant-containing amorphous solid dispersions: Orthogonal analytical methods to probe the effects of surfactants on morphology and phase composition. Int J Pharm. 2022;619:121708. https://doi.org/10.1016/j.ijpharm.2022.121708

[16] Luebbert C, Wessner M, Sadowski G. Mutual impact of phase separation/crystallization and water sorption in amorphous solid dispersions. Mol Pharm. 2018;15(2):669-678. https://doi.org/10.1021/acs.molpharmaceut.7b01076

[17] Zeng A, Yao X, Gui Y, Li Y, Jones KJ, Yu L. Inhibiting surface crystallization and improving dissolution of amorphous loratadine by dextran sulfate nanocoating. J Pharm Sci. 2019;108(7):2391-2396. https://doi.org/10.1016/j.xphs.2019.02.018

[18] Bhujbal SV, Mitra B, Jain U, Gong Y, Agrawal A, Karki S, Taylor LS, Kumar S, Tony Zhou Q. Pharmaceutical amorphous solid dispersion: A review of manufacturing strategies. Acta Pharm Sin B. 2021;11(8):2505-2536. https://doi.org/10.1016%2Fj.apsb.2021.05.014

[19] Mendonsa N, Almutairy B, Kallakunta VR, Sarabu S, Thipsay P, Bandari S, Repka MA. Manufacturing strategies to develop amorphous solid dispersions: An overview. J Drug Deliv Sci Technol. 2020;55:101459. https://doi.org/10.1016%2Fj.jddst.2019.101459

[20] Saha SK, Joshi A, Singh R, Jana S, Dubey K. An investigation into solubility and dissolution improvement of alectinib hydrochloride as a third-generation amorphous solid dispersion. J Drug Deliv Sci Technol. 2023;81:104259. http://dx.doi.org/10.1016/j.jddst.2023.104259

[21] Singh A, Van den Mooter G. Spray drying formulation of amorphous solid dispersions. Adv Drug Del Rev. 2016;100:27-50. https://doi.org/10.1016/j.addr.2015.12.010

[22] Mishra DK, Dhote V, Bhargava A, Jain DK, Mishra PK. Amorphous solid dispersion technique for improved drug delivery: Basics to clinical applications. Drug Deliv Transl Res. 2015;5:552-565. https://doi.org/10.1007/s13346-015-0256-9

[23] Shi X, Xu T, Huang W, Fan B, Sheng X. Stability and bioavailability enhancement of telmisartan ternary solid dispersions: the synergistic effect of polymers and drug-polymer (s) interactions. AAPS PharmSciTech. 2019;20(4):143. https://doi.org/10.1208/s12249-019-1358-3

[24] Thompson SA, Davis Jr DA, Miller DA, Kucera SU, Williams III RO. Pre-processing a polymer blend into a polymer alloy by KinetiSol enables increased ivacaftor amorphous solid dispersion drug loading and dissolution. Biomedicines. 2023;11(5):1281. https://doi.org/10.3390/biomedicines11051281

[25] Li J, Wang Y, Yu D. Effects of additives on the physical stability and dissolution of polymeric amorphous solid dispersions: a Review. AAPS PharmSciTech. 2023;24(7):175. https://doi.org/10.1208/s12249-023-02622-8

[26] Kourounakis AP, Xanthopoulos D, Tzara A. Morpholine as a privileged structure: A review on the medicinal chemistry and pharmacological activity of morpholine containing bioactive molecules. Med Res Rev. 2020;40(2):709-752. https://doi.org/10.1002/med.21634
[27] Mesallati H, Umerska A, Paluch KJ, Tajber L. Amorphous polymeric drug salts as ionic solid dispersion forms of ciprofloxacin. Mol Pharm. 2017;14(7):2209-2223. https://doi.org/10.1021/acs.molpharmaceut.7b00039
[28] Crucitti VC, Migneco LM, Piozzi A, Taresco V, Garnett M, Argent RH, Francolini I. Intermolecular interaction and solid state characterization of abietic acid/chitosan solid dispersions possessing antimicrobial and antioxidant properties. Eur J Pharm Biopharm. 2018;125:114-123. https://doi.org/10.1016/j.ejpb.2018.01.012
[29] Kumar N, Sarup P, Pahuja S. Formulation and characterization of dispersible tablets of cefpodoxime proxetil: A cephalosporin antibiotic. Res J Pharm Technol. 2021; 14(5):2806-2813. https://doi.org/10.52711/0974-360X.2021.00495
[30] Mostafa GA, Al-Otaibi YH, Al-Badr AA. Cefpodoxime proxetil. Profiles Drug Subst Excip Relat Methodol. 2019;44:1-165. https://doi.org/10.1016/bs.podrm.2019.02.001
[31] Patil P, Suryawanshi S, Patil S, Pawar A. HME-assisted formulation of taste-masked dispersible tablets of cefpodoxime proxetil and roxithromycin. J Taibah Univ Med Sci. 2023;19(2):252-262. https://doi.org/10.1016/j.jtumed.2023.12.004
[32] Jindal A, Kumar A. Physical characterization of clove oil based self Nano-emulsifying formulations of cefpodoxime proxetil: Assessment of dissolution rate, antioxidant & antibacterial activity. OpenNano. 2022;8:100087. https://doi.org/10.1016/j.onano.2022.100087
[33] Mujtaba A, Ali M, Kohli K. Statistical optimization and characterization of pH-independent extended-release drug delivery of cefpodoxime proxetil using Box–Behnken design. Chem Eng Res Des. 2014;92(1):156-165. http://dx.doi.org/10.1016/j.cherd.2013.05.032
[34] Patil SH, Talele GS. Natural gum as mucoadhesive controlled release carriers: evaluation of cefpodoxime proxetil by D-Optimal design technique. Drug Deliv. 2014;21(2):118-129. https://doi.org/10.3109/10717544.2013.834416
[35] Alipour A, Babaei Shekardasht M, Gharbani P, Mirzaei Shalmani M. Synthesis, characterization and application of MP@ p (EGDMA-co-HPMA) in adsorption and release of cefpodoxime. Int J Polym Mater Polym Biomater. 2023:73(9):1-10. http://dx.doi.org/10.1080/00914037.2023.2207138
[36] Kakumanu VK, Arora V, Bansal AK. Investigation on physicochemical and biological differences of cefpodoxime proxetil enantiomers. Eur J Pharm Biopharm. 2006;64(2):255-259. https://doi.org/10.1016/j.ejpb.2006.05.001
[37] Li J, Zhang D, Hu C. Characterization of impurities in cefpodoxime proxetil using LC–MSn. Acta Pharm Sin B. 2014;4(4):322-332. https://doi.org/10.1016%2Fj.apsb.2014.06.007
[38] Nappinnai M, Sivaneswari S. Formulation optimization and characterization of gastroretentive cefpodoxime proxetil mucoadhesive microspheres using 32 factorial design. J Pharm Res. 2013;7(4):304-309. http://dx.doi.org/10.1016/j.jopr.2013.04.014
[39] Kakumanu VK, Arora V, Bansal AK. Investigation of factors responsible for low oral bioavailability of cefpodoxime proxetil. Int J Pharm. 2006;317(2):155-160. https://doi.org/10.1016/j.ijpharm.2006.03.004
[40] Fukutsu N, Kawasaki T, Saito K, Nakazawa H. Application of high-performance liquid chromatography hyphenated techniques for identification of degradation products of cefpodoxime proxetil. J Chromatogr A. 2006;1129(2):153-159. https://doi.org/10.1016/j.chroma.2006.06.102
[41] Hamaura T, Kusai A, Nishimura K. Gel formation of cefpodoxime proxetil. STP Pharma Sci. 1995;5(4):324-331.
[42] Hamamura T, Ohtani T, Kusai A, Nishimura K. Unusual dissolution behavior of cefpodoxime proxetil: effect of pH and ionic factors. STP Pharm Sci. 1995;5:332-338.
[43] Chu J, Li G, Row KH, Kim H, Lee Y-W. Preparation of cefpodoxime proxetil fine particles using supercritical fluids. Int J Pharm. 2009;369(1-2):85-91. https://doi.org/10.1016/j.ijpharm.2008.10.029
[44] Crauste-Manciet S, Huneau J, Decroix M, Tome D, Farinotti R, Chaumeil J. Cefpodoxime proxetil esterase activity in rabbit small intestine: a role in the partial cefpodoxime absorption. Int J Pharm. 1997;149(2):241-249. https://doi.org/10.1016/S0378-5173(97)04881-3
[45] Heng W, Wei Y, Xue Y, Cheng H, Zhang L, Zhang J, Gao Y, Qian S. Gel formation induced slow dissolution of amorphous indomethacin. Pharm Res. 2019;36:1-14. https://doi.org/10.1007/s11095-019-2700-x
[46] Yurtdaş-Kırımlıoğlu G. Development and characterization of lyophilized cefpodoxime proxetil-Pluronic® F127/polyvinylpyrrolidone K30 solid dispersions with improved dissolution and enhanced antibacterial activity. Pharm Dev Technol. 2021;26(4):476-489. https://doi.org/10.1080/10837450.2021.1889584
[47] Sharma N, Jain N, Sudhakar C, Jain S. Formulation and evaluation of gastro retentive floating tablets containing cefpodoxime proxetil solid dispersions. Int J Curr Pharm Res. 2012;4(4):82-87.
[48] Mujtaba A, Ali M, Kohli K. Formulation of extended release cefpodoxime proxetil chitosan–alginate beads using quality by design approach. Int J Biol Macromol. 2014;69:420-429. https://doi.org/10.1016/j.ijbiomac.2014.05.066
[49] Patil PS, Suryawanshi SJ, Patil SS, Pawar AP. HME-assisted formulation of taste-masked dispersible tablets of cefpodoxime proxetil and roxithromycin. J Taibah Univ Med Sci. 2024;19(2):252-262. https://doi.org/10.1016%2Fj.jtumed.2023.12.004
[50] Apiwongngam J, Limwikrant W, Jintapattanakit A, Jaturanpinyo M. Enhanced supersaturation of chlortetracycline hydrochloride by amorphous solid dispersion. J Drug Deliv Sci Technol. 2018;47:417-426. http://dx.doi.org/10.1016/j.jddst.2018.08.007

[51] Shehab OR, AlRabiah H, Abdel-Aziz HA, Mostafa GA. Charge-transfer complexes of cefpodoxime proxetil with chloranilic acid and 2, 3-dichloro-5, 6-dicyano-1, 4-benzoquinone: Experimental and theoretical studies. J Mol Liq. 2018;257:42-51. http://dx.doi.org/10.1016/j.molliq.2018.02.083

[52] Kader NA, Kamer AA, Elekhnawy E, Arafa M, Essa EA, El Maghraby GM. Melt granulation for enhanced dissolution rate and antimicrobial activity of cefpodoxime proxetil. Res J Pharm Technol. 2023;16(8):3921-3928. http://dx.doi.org/10.52711/0974-360X.2023.00645

[53] Duraivel S, Venkateswarlu V, Kumar AP, Gopinath H. Enhancement of dissolution rate of cefpodoxime proxetil by using solid dispersion and cogrinding approaches. Res J Pharm Technol. 2012;5(12):1552-1562.

[54] Fan Y, Chen H, Huang Z, Zhu J, Wan F, Peng T, Pan X, Huang Y, Wu C. Taste-masking and colloidal-stable cubosomes loaded with Cefpodoxime proxetil for pediatric oral delivery. Int J Pharm. 2020;575:118875. https://doi.org/10.1016/j.ijpharm.2019.118875

[55] Gupta MK, Vanwert A, Bogner RH. Formation of physically stable amorphous drugs by milling with Neusilin. J Pharm Sci. 2003;92(3):536-551. https://doi.org/10.1002/jps.10308

[56] Ivanisevic I. Physical stability studies of miscible amorphous solid dispersions. J Pharm Sci. 2010;99(9):4005-4012. https://doi.org/10.1002/jps.22247

[57] Sahoo A, Kumar NK, Suryanarayanan R. Crosslinking: An avenue to develop stable amorphous solid dispersion with high drug loading and tailored physical stability. J Control Release. 2019;311:212-224. https://doi.org/10.1016/j.jconrel.2019.09.007

[58] Kaur S, Jena SK, Samal SK, Saini V, Sangamwar AT. Freeze dried solid dispersion of exemestane: A way to negate an aqueous solubility and oral bioavailability problems. Eur J Pharm Sci. 2017;107:54-61. https://doi.org/10.1016/j.ejps.2017.06.032

[59] Mujtaba A, Kohli K. In vitro/in vivo evaluation of HPMC/alginate based extended-release matrix tablets of cefpodoxime proxetil. Int J Biol Macromol. 2016;89:434-441. https://doi.org/10.1016/j.ijbiomac.2016.05.010

[60] Luebbert C, Sadowski G. Moisture-induced phase separation and recrystallization in amorphous solid dispersions. Int J Pharm. 2017;532(1):635-646. https://doi.org/10.1016/j.ijpharm.2017.08.121

[61] Moseson DE, Parker AS, Beaudoin SP, Taylor LS. Amorphous solid dispersions containing residual crystallinity: Influence of seed properties and polymer adsorption on dissolution performance. Eur J Pharm Sci. 2020;146:105276. https://doi.org/10.1016/j.ejps.2020.105276

[62] Newman A, Knipp G, Zografi G. Assessing the performance of amorphous solid dispersions. J Pharm Sci. 2012;101(4):1355-1377. https://doi.org/10.1002/jps.23031

[63] Aldafaay AAA, Abdulamir HA, Abdulhussain HA, Badry AS, Abdulsada AK. The use of Urinary α-amylase level in a diagnosis of chronic renal failure. Res J Pharm Technol. 2021; 14(3):1597-1600. http://dx.doi.org/10.5958/0974-360X.2021.00283.3

[64] Al-Shammari AH, Abbood ZA, Lateef HF. Assessing the impacts of L-carnitine and modafinil on fatigue in Iraqi multiple sclerosis patients. J Adv Pharm Technol Res. 2023;14(3):226-228. https://doi.org/10.4103%2FJAPTR.JAPTR_225_23